Journal of Non-Crystalline Solids 354 (2008) 4887–4893

Contents lists available at ScienceDirect

Journal of Non-Crystalline Solids

journal homepage: www.elsevier.com/locate/jnoncrysol

# Synthesis and characterization of phosphate glass microspheres for radiotherapy applications

Frank F. Sene [a], José R. Martinelli [a,*], Emico Okuno [b]

[a] Nuclear and Energy Research Institute, IPEN – CCTM, Caixa Postal 11049, Pinheiros, 05422-970 Sao Paulo, SP, Brazil
[b] Physics Institute of University of Sao Paulo, Brazil

ARTICLE INFO

*Article history:*
Available online 25 August 2008

*PACS:*
81.05.kf
87.53.Ju

*Keywords:*
Biomaterials
Chemical durability
Phosphates

ABSTRACT

Glass microspheres containing the radioisotope $^{32}P$, a $\beta^-$ particle emitter, and half-life of 14.3 days, can be easily introduced in specific human organs such as liver, pancreas, and uterus to kill cancer cells. In the present work phosphate glass microspheres were produced with different compositions and particle size distribution in the range of 20– 30 μm. Two different thermal processes were used to spherodize glass particles originally with irregular shapes. Samples were characterized by X-rays diffraction to check the amorphous structure, energy dispersive X-rays fluorescence spectroscopy to determine the final glass composition, and Fourier transformed infrared spectroscopy to determine the structural groups in the glass structure. The dissolution rate of glass samples in water was determined at 90 °C, and in simulated body fluid (SBF) at 37 °C. Glasses with dissolution rates close to $10^{-5}$ g/(cm$^2$ day) were obtained, which make them suitable for the present application. Scanning electron microscopy was used to evaluate the shape of the microspheres before and after the dissolution tests. The cytotoxicity tests showed that these microspheres can be used for biological applications.



## 1. Introduction

Radiotherapy is an alternative way for cancer treatment [1]. Brachytherapy is a technique that introduces the radioactive source directly in the human body, permanently or temporally [2]. A promising brachytherapy technique uses glass microspheres to carry the radioactive source. The spherical shape and the chemical resistance of the glass particles make them a promising material for liver cancer treatment. Avoiding sharp edges of glass particles reduces the damage of healthy tissues and unnecessary hemorrhage [3].

Some types of cancers are difficult to be treated, and liver cancer is one of them. Generally it is terminal, and after being diagnosed the patient's life expectancy is only a few months. Surgery is an option that is seldom used due to the high probability of causing metastases. Chemotherapy might offer a temporary relief however it is often suspended before eliminating all the malign cells, aggravating the clinical condition of the patient. On the other hand, radiotherapy treatments that use external radiation sources, such as teletherapy, do excessive harm to the neighboring healthy tissues. The dose applied in multiple plans and steps intends to minimize the side effects related to the irradiation; however, it is still not enough to precisely restrict the irradiated area to the cancer tissues without damaging a large area of healthy tissues. Usually this treatment requires an average of 10 irradiations in a period of 30 days with doses of approximately 2500 rads. On the other hand, if the radiation source is localized as in the brachytherapy, doses of up to 15,000 rads can be used in a single step, been enough to kill cancer cells without damaging significantly the healthy neighboring tissues [3–5]. The use of $\beta^-$ particles is an additional advantage over the $\gamma$ rays. The short penetration range of those particles allows an effective energy absorption in the restricted area of the tumor to be treated. Glass microspheres of $17Y_2O_3$–$19Al_2O_3$–$64SiO_2$ (mol%) with sizes in the range of 20–40 μm have been used in cancer brachytherapy treatments [3–5]. The isotope $^{89}Y$ is transmuted to $^{90}Y$ by neutron activation resulting in a $\beta^-$ emitter with half-life of 64.1 h [6]. Other elements that are part of the glass structure, such as $^{27}Al$, and $^{30}Si$, are also activated becoming $\beta^-$ emitters; however, the half-life is only 2.25 min and 2.62 h, respectively [6]. These microspheres are chemically resistant to body fluids and are non-cytotoxic [7]. After the neutron activation, these microspheres are injected in the liver through the hepatic artery, restricting a relative high radiation dose only in the tumor [3–5]. These glasses were submitted to clinical testes for treatment of cancer in liver and kidney, as well for synovectomy [7–15]. Similarly to the isotope $^{89}Y$, the isotope $^{31}P$ can be transmuted to $^{32}P$ which is $\beta^-$ emitter with a half-life of 14.3 days and can be more effective to cancer treatment when compared

* Corresponding author. Tel.: +55 11 3133 9208; fax: +55 11 3133 9276.
*E-mail address:* jroberto@ipen.br (J.R. Martinelli).

0022-3093/$ - see front matter © 2008 Elsevier B.V. All rights reserved.
doi:10.1016/j.jnoncrysol.2008.04.041

to $^{90}Y$. In a previous work $P^+$ ions were implanted in $Y_2O_3$–$Al_2O_3$–$SiO_2$ glasses showing promising results [16]. However, phosphorus can be a problem in some types of glasses because it usually plays an important role in the nucleation of crystalline phases, as observed for some silicate glasses.

The specific activities for the radionuclides $^{90}Y$ and $^{32}P$ are 92.5 GBq/g and 66.6 GBq/g, respectively. The cross-sections for neutron absorption reaction, $\sigma_n$, for $^{89}Y$ and $^{31}P$ are $1.28 \times 10^{-24}$ and $0.17 \times 10^{-24}$ cm$^2$, respectively, making necessary longer radiation times for glass microspheres containing phosphorus when compared to yttrium. However, the amount of phosphorus in the glass microspheres is usually higher when compared to yttrium in similar microspheres. This fact compensates the lower cross section of P and leads to microspheres which activity is suitable for radiotherapic treatments.

The majority of phosphate glasses are relatively easy to be obtained at melting temperatures in the range of 900–1300 °C. In the present work aluminophosphate glasses containing silica and magnesia, which require melting temperatures in the range of 1250–1550 °C, were prepared and further used to obtain glass microspheres.

## 2. Experimental procedures

Glasses based on the compositions showed in Table 1 were prepared by mixing analytical grade $(NH_4)_2HPO_4$, $Al_2O_3$, MgO, and $SiO_2$, melted in an electric furnace in the temperature range of 1250–1550 °C for 2 h, stirred each 30 min with a high purity silica rod to achieve a homogeneous melt. After casting, the material was ground in stainless steal ball milling and sieved to separate particles in the size range of 20–50 μm. A $10 \times 10 \times 1$ mm$^3$ piece was used for leaching tests in water and simulated body fluid (SBF). The amount of $SiO_2$ and $Al_2O_3$ were varied to evaluate the effects on the chemical durability in the final glass composition. Not all compositions described in Table 1 were tested, because some of them were preliminarily identified as having relatively low chemical resistance in water; then, only the promising compositions were tested.

Glass particles with irregular shapes were transformed to microspheres by using two different processes. In the first process, glass microspheres with particle size distribution in the range of 20–150 μm were obtained by re-melting irregular particles in a hot flame. A torch burning a mixture of oxygen and petrol liquefied gas was used for this purpose. The microspheres were collected in a metal cylinder. Although this process has been previously reported [17] and it is known as 'spheronization by flame', for each type of glass the experimental parameters had to be adjusted to reach the best results. The second process consists of introducing glass particles with irregular shapes on the top of a vertical tubular furnace, and allowing them to fall down inside the furnace. This process is now named 'spheronization by gravitational fall in a tubular furnace'.

**Table 1**
Nominal glass composition (wt %).

| Glass type | $P_2O_5$ | $Al_2O_3$ | $SiO_2$ | MgO |
|---|---|---|---|---|
| MVP1 | 60 | 15 | 15 | 10 |
| MVP2 | 60 | 10 | 15 | 15 |
| MVP3 | 60 | 10 | 10 | 20 |
| MVP5 | 60 | 10 | 5 | 25 |
| MVP6 | 40 | 5 | 5 | 30 |
| MVP8a | 45 | 5 | 5 | 45 |
| MVP8b | 43 | 4 | 10 | 43 |
| MVP8c | 42 | 4 | 12 | 42 |
| MVP9a | 41 | 3 | 15 | 41 |
| MVP9b | 42 | 10 | 4 | 44 |
| MVP9c | 42 | 12 | 4 | 42 |
| MVP9d | 41 | 15 | 3 | 41 |

Samples were characterized by X-rays diffraction (XRD), differential thermal analysis (DTA), energy dispersive X-rays analysis (EDX) coupled to a scanning electron microscope or by using an EDX (Shimadzu model 720). Scanning electron microscopy was used to observe glass samples before and after being exposed to a simulated body fluid (SBF).

Samples $10 \times 10 \times 1$ mm$^3$ were immersed in 100 ml of SBF at 37 °C during 21 days. The sample's weight was monitored after 1, 3, 7, and 14 days. All measurements were replicate with three different samples and the results presented are an average of these data.

Glass samples were tested 'in vitro' to evaluate the toxic effects on cells by using a diluted extract of the material in contact with cells of Chinese Hamster Ovarian (CHO), American Type Culture Collection (ATCC) (IS0 10993-5, 1992) [18–19].

Infrared spectroscopy with Fourier transform (FTIR) (Thermo Nicolet, model Nexus 670) was performed to evaluate the surface hygroscopicity, the presence of hydroxyl groups in the glass, to identify the chemical bonds between the glass formers, and how the modifiers affect the glass structure. Samples were prepared by mixing 2 wt% of glass particles (average particle size of 10 μm) with KBr (dehydrated), uniaxially pressed to obtain a pellet with 12 mm in diameter and 0.5 mm thickness.

## 3. Results

### 3.1. X-ray diffraction and differential thermal analysis

Fig. 1 shows the XRD patterns for microspheres with composition MVP3, MVP8c, and MVP9c.

Figs. 2–4 show the XRD patterns for microspheres with different compositions after heat treatment at a specific temperature for 2 h. The temperature was chosen based on the maximum crystallization temperature determined from the DTA curves.

### 3.2. Differential thermal analysis (DTA) and thermogravimetry (TG)

Fig. 5 shows the DTA curve for the MVP1 glass. Other glasses such as MPV3, MVP5, and MVP6 show similar curves.

Fig. 6(a) and (b) shows the DTA and TG curves for MVP8, and MVP9 glasses. Table 2 presents the $T_g$ and $T_c$ values determined from those curves.

### 3.3. Fourier transform infrared spectroscopy (FTIR)

Fig. 7 shows the FTIR spectra for MVP3, MVP8a, and MVP8d glasses.

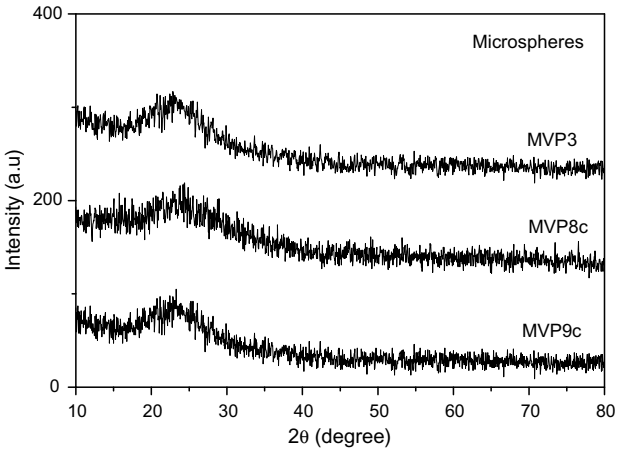


**Fig. 1.** XRD patterns for microspheres with compositions MVP3, MVP8c, and MVP9c.

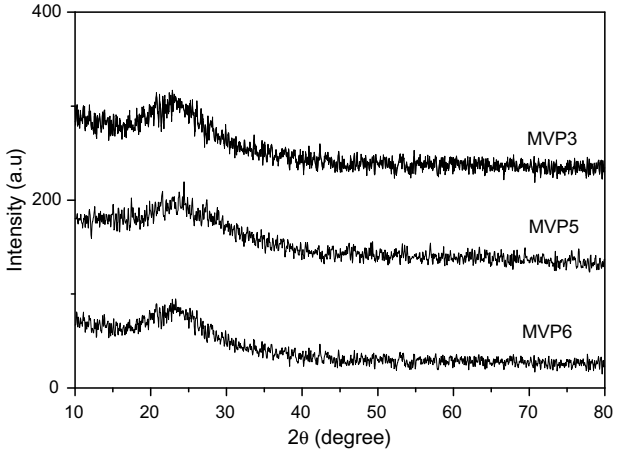


**Fig. 2.** XRD pattern for microspheres with compositions MVP3, MVP5, and MVP6 after heat treatment.

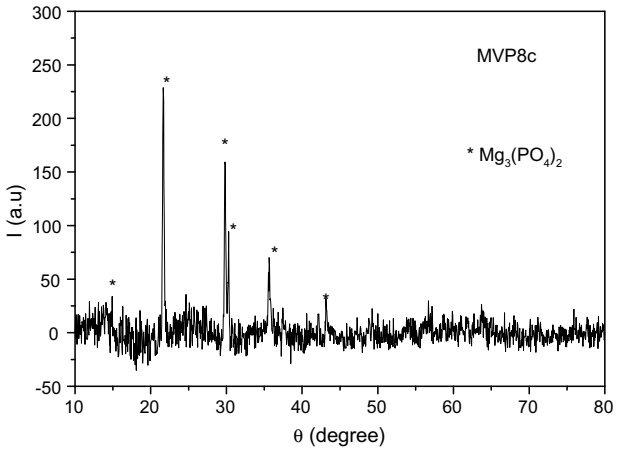


**Fig. 3.** XRD pattern for microspheres with compositions MVP8c, after heat treatment.

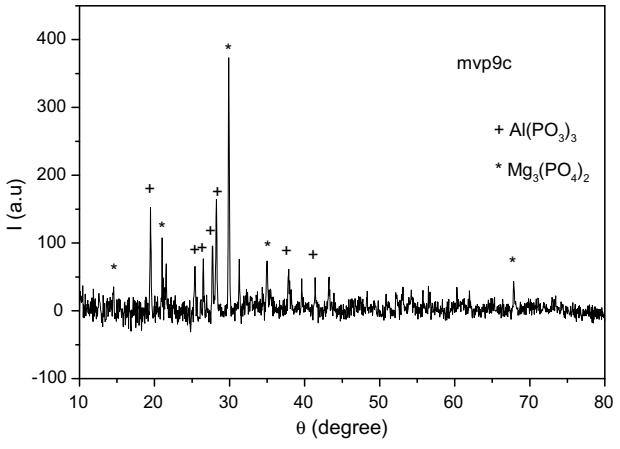


**Fig. 4.** XRD pattern for microspheres with compositions MVP9c, after heat treatment.

### 3.4. Energy dispersive X-Rays analysis (EDX) and dissolution rate (DR)

Table 3 presents the amount of phosphorus for the MVP3, MVP8, and MVP9 glasses determined by EDX.

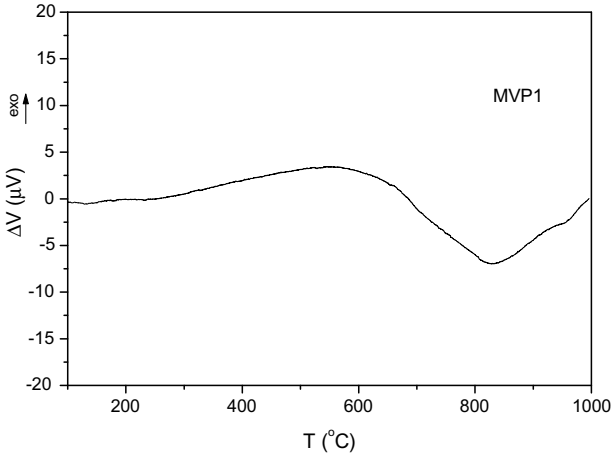


**Fig. 5.** DTA curve for MVP1.

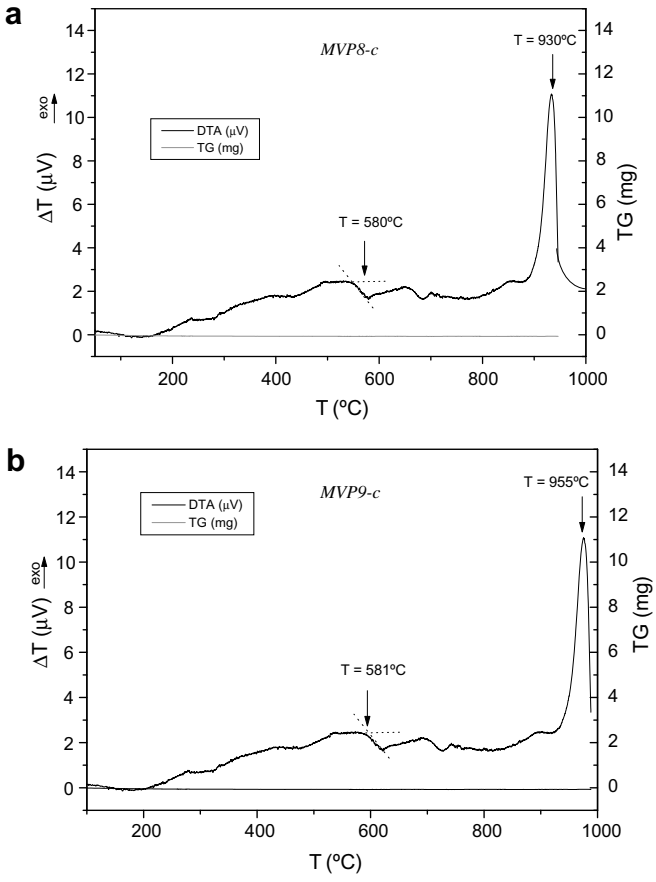


**Fig. 6.** DTA curves for:(a) MVP8-c, and (b) MVP9-c.

**Table 2**
Values of $T_g$ and $T_c$ for some glasses

| Glass type | $T_g$ (°C) | $T_c$ (°C) |
|---|---|---|
| MVP8c | 580 ± 5 | 930 ± 5 |
| MVP9c | 581 ± 5 | 955 ± 5 |

Table 4 presents the surface glass composition of the MVP3 and MVP9c glasses (the initial composition and after 28 days immersed in SBF at 37 °C), determined by EDX.

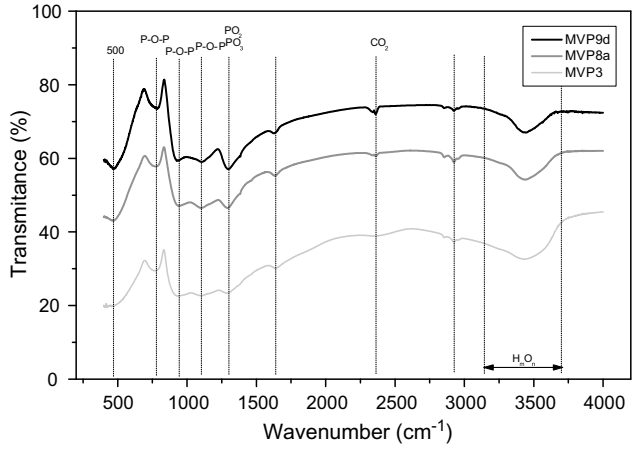


**Fig. 7.** FTIR spectra for glasses MVP3, MVP8, and MVP9.

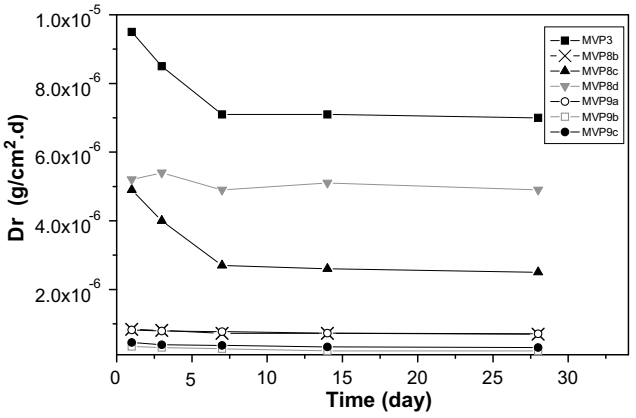


**Fig. 8.** Dissolution rate (Dr) as a function of immersion time in distilled water at 90 °C. Data error is estimated to be 2%.

**Table 3**
Phosphorus concentration in glass microspheres

| Glass type | P (at.%) |
|---|---|
| MVP3 | 43.8 |
| MVP8b | 37.8 |
| MVP8c | 38.2 |
| MVP9c | 32.6 |

**Table 4**
Surface glass composition after immersion in SBF at 37 °C as a function of immersion time

| *t* (day) | wt% | | | |
|---|---|---|---|---|
| | $P_2O_5$ | $SiO_2$ | $Al_2O_3$ | MgO |
| (a) | | | | |
| 0 | 62.70 ± 0.2 | 9.70 ± 0.1 | 10.08 ± 0.1 | 17.55 ± 0.2 |
| 28 | 62.52 ± 0.2 | 9.69 ± 0.1 | 10.02 ± 0.1 | 17.18 ± 0.2 |
| (b) | | | | |
| 0 | 38.12 ± 0.2 | 4.22 ± 0.1 | 17.21 ± 0.1 | 40.39 ± 0.2 |
| 28 | 38.50 ± 0.2 | 4.29 ± 0.1 | 17.28 ± 0.1 | 40.72 ± 0.2 |

(a) MVP3 and (b) MVP9c.

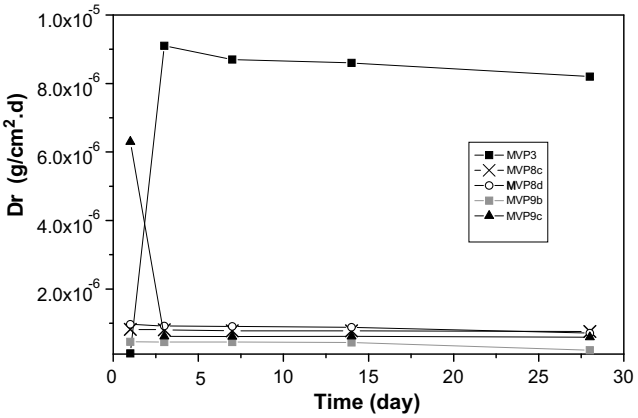


**Fig. 9.** Dissolution rate (Dr) as a function of immersion time in SBF at 37 °C. Data error is estimated to be 2%.

Fig. 8 presents the dissolution rate for glasses immersed in distilled water at 90 °C. Fig. 9 presents the dissolution rate for glasses immersed in SBF at 37 °C. Since these glass samples were $10 \times 10 \times 1$ mm$^3$ blocks, they were previously annealed at 580 °C.

### 3.5. Scanning electron microscopy

Fig. 10(a) shows the micrograph of glass particles with irregular shapes originally used to prepare glass microspheres. Fig. 10(b)–(d) shows the micrographs of microspheres with composition MVP3 (different magnifications are shown in the figures). Fig. 11(a) and (b) shows the micrographs of microspheres with composition MVP9c.

Fig. 12(a) and (b) shows the scanning electron micrographs of microspheres with composition MVP3 and MVP9b after withdrawing from a bath containing SBF during 21 days at 37 °C, and dried afterwards. Fig. 12(c) and (d) shows the same micrographs but with higher magnification.

### 3.6. Cytotoxicity tests

Fig. 13 presents the results of the cytotoxicity tests performed by the method of neutral red incorporation.

## 4. Discussion

### 4.1. X-ray diffraction (XRD)

From Fig. 1, it is noticed that these glasses are very stable and do not show any evidence of crystalline phases after being spheronized. Frequently the nucleation of crystalline phases is undesirable because it can induce stresses in the glass structure and interfere in the performance of the microspheres by creating cracks and other defects.

From Figs. 2–4 it is noticed according to the XRD patterns that the compositions MVP3, MVP5, and MVP6 are very resistant to crystallization. No evidence of crystalline phases is observed after a heat treatment. However, microspheres with composition MVP8c, and MVP9c present XRD patterns with some diffraction peaks that can be assigned to crystalline phases. This phase transformation occurs at time periods longer than the ones necessary for the spheronization, and therefore, either the number of nuclei or the growth of them can be neglected in this process.

### 4.2. Differential thermal analysis (DTA)

From Fig. 5 it can be noticed that there is no exothermic peak that could be assigned to a crystallization process for glasses with composition MVP1. This result is in agreement with the XRD results and we can infer that these glasses are very resistant to crystallization. From Fig. 6(a) and (b), and Table 2, it can be noticed that

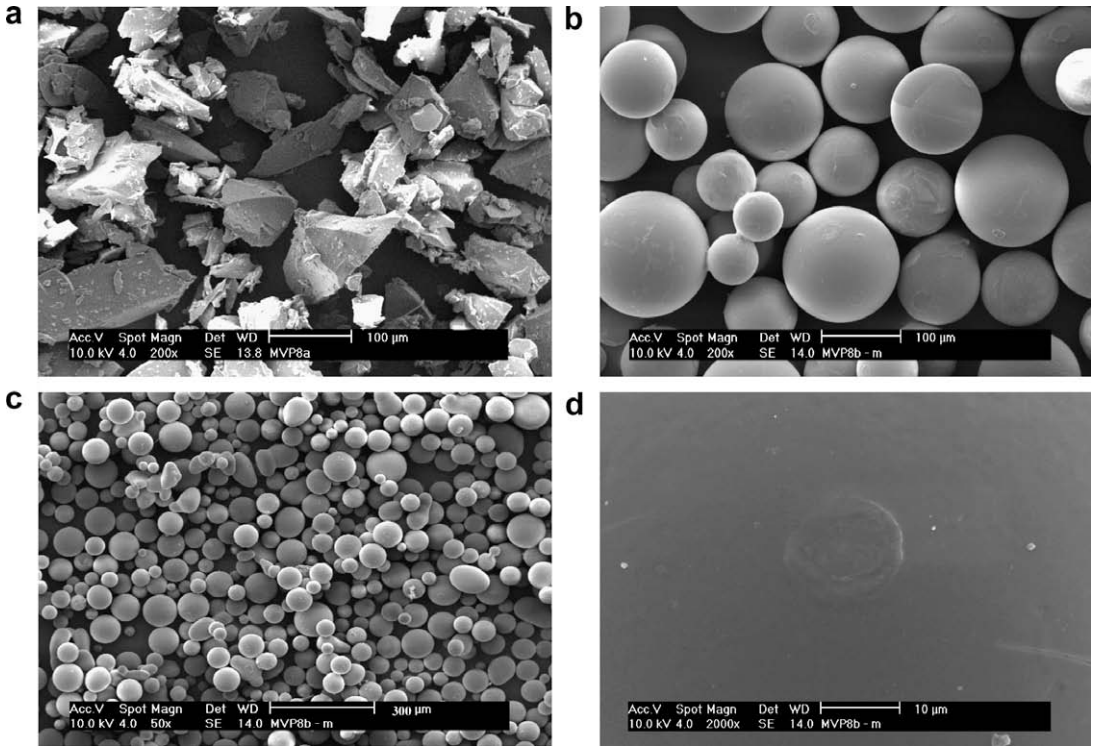


**Fig. 10.** Scanning electron micrographs of: (a) glass powders used to obtain microspheres , (b), (c) and (d) microspheres with composition MVP3 (different magnifications).

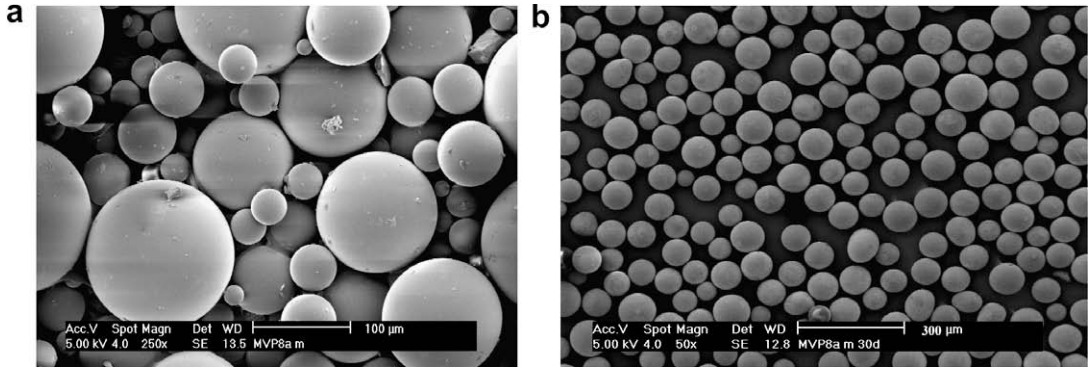


**Fig. 11.** Scanning electron micrographs of microspheres with composition MVP9c (different magnification).

the glasses MVP8c and MVP9c present an exothermic peak that could be assigned to a crystallization process.

To significantly reduce the residual stresses in glass pieces that were used to evaluate the chemical resistance, the annealing temperature was chosen based on the $T_g$ values. Usually it is chosen a temperature 10 °C higher than $T_g$. The annealing time is 2 h to reduce the residual stress caused by the cooling procedure.

### 4.3. Fourier transform infrared spectroscopy (FTIR)

The spectra presented in Fig. 7 are similar to the ones previously reported for different phosphate glasses [20,21]. The absorption band at 500 $cm^{-1}$ can be assigned to vibration modes of $P_2O_7$ groups superimposed to stretching vibrations of P–O–Mg and P–O–Al bonds, and the intensity increases as the amount of MgO or $Al_2O_3$ increases [22]. The increase of chemical durability is related to the presence of Al and Mg. The absorption band at 760 $cm^{-1}$ can be assigned to symmetric stretching modes of P–O–P bonds [23] and the band at 923 $cm^{-1}$ to asymmetric stretching modes of P–O–P bonds. The band located in the range 1250–1320 $cm^{-1}$ is assigned to asymmetric stretching modes of terminal groups $(PO_2)^-$ and $(PO_3)^{2-}$ , respectively [20].

An absorption band around 3250 $cm^{-1}$ is related to stretching modes of O–H. A band located at 3250 $cm^{-1}$ was expected, however the presence of $H_mO_n$ groups (structural water) contributes to the formation of a shoulder in that region [24]. The intensity of this band decreases as the amount of $P_2O_5$ decreases and as the amount of MgO and $Al_2O_3$ increases. Therefore MVP8 glasses are less susceptible to be attacked by the environmental humidity. Further chemical durability tests will confirm this assumption.

A low intensity absorption band located at 2370 $cm^{-1}$ is assigned to $CO_2$ in the glass structure [20]. The estimated amount of $CO_2$ is very low because the major contribution to the absorption coefficient in this wavenumber is related to the absorption due to the stretching modes of OH in the $H_mO_n$ groups [25,26].

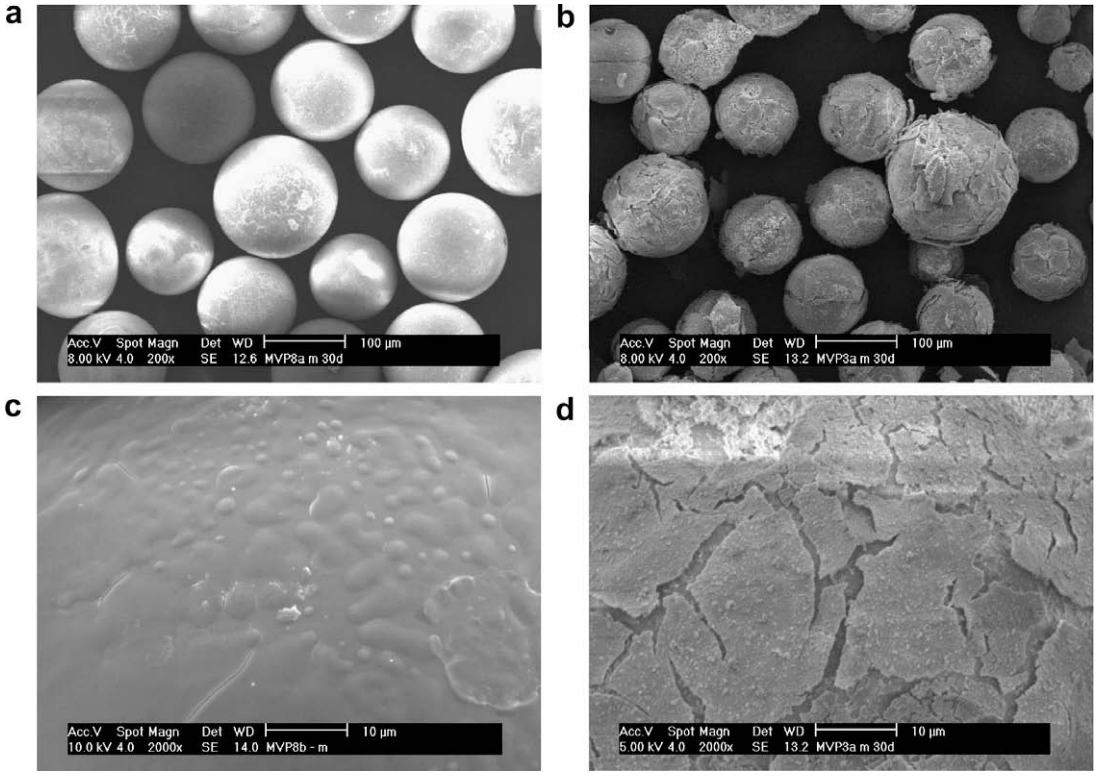


**Fig. 12.** Microspheres after withdrawing from a bath containing SBF at 37 °C during 21 days (a) and (c) MVP9b; (b) and (d) MVP3.

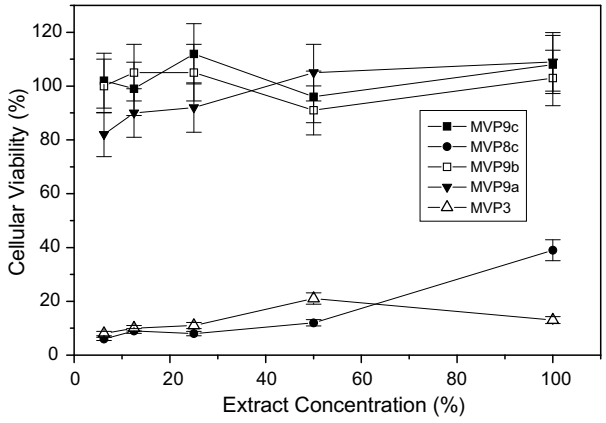


**Fig. 13.** Cellular viability of glass samples as a function of the extract concentration.

### 4.4. Energy dispersive X-rays analysis (EDX) and dissolution rate (DR)

Table 3 presents the amount of phosphorus in the MVP3, MVP8, and MVP9 glasses determined by EDX. These results can be useful to estimate the activity of microspheres and the absorbed dose. By comparing the amount of phosphorus with the batch composition presented in Table 1, and making a simple ratio between the amount of $P_2O_5$ and the at.% of P, it is noticed that the P loss for MVP3 glass is higher than the one for the other glass types in Table 3.

From Table 4 it is noticed that the variation among the glass constituents during the leaching procedure is small. These results complement the ones obtained to determine the chemical durability by weight loss. Since the MVP9c glass has a chemical durability superior than the one for the MVP3 glass, it is assumed that there was not a selective leaching of the elements. These results can also be useful in the future to estimate the activity of microspheres and the absorbed dose.

From Figs. 8 and 9, it is noticed that the MVP9b composition has the highest corrosion resistance either in water or in SBF. In a preliminary work it was noticed that the glass types MVP1, MVP2, MVP5, and MVP6 are not chemically resistant when immersed in water at 90 °C, so they were discarded for further investigation.

All samples show a decreasing dissolution rate as a function of time which is related to the decrease of mass transfer from the glass to the medium. This fact might be related to the precipitation of secondary phases on the glass surface or to the saturation of the leaching solution with the corroded elements. In any case, these glasses have a higher chemical durability than commercial window glasses (DR = $10^{-5}$ g/cm$^2$ day).

### 4.5. Electron scanning microscopy

In all cases the shapes are regular and very close to spheres (Figs. 10 and 11). Therefore the procedure to obtain this material is appropriated. These micrographs will be used to determine the average particle size after processing the images.

Based on the low corrosion attack by the SBF (Fig. 12), it is assumed that MVP9b microspheres are a promising material for the application proposed in the present work. On the other hand, MVP3 microspheres present some undesirable features. These results are in agreement with the chemical durability tests either in SBF or in water.

### 4.6. Cytotoxicity tests

Based on the cytotoxicity tests presented in Fig. 13, microspheres with composition MVP9a, MVP9b, and MVP9c are suitable for the application aimed at this work, however the MVP3 and

MVP8c microspheres are inadequate because they can initiate an inflammatory process and, consequently, the cellular tissue necrosis. The inadequacy of MVP3 might be related to the high dissolution of glass elements, since this material presents a lower chemical durability compared to the MVP9b and MVP9c. The MVP8c glass has a relatively high chemical durability; however the low cellular viability is due to the dissolution of silicon and phosphorus, which, even in low concentrations, can affect the cellular viability. This problem was solved by changing the composition to the MVP9, with higher amounts of $Al_2O_3$ and consequently the decrease of the dissolution rates of all glass constituents.

## 5. Conclusions

Glass microspheres with different compositions and resistant to crystallization were obtained with size and shapes appropriated to brachytherapy applications. The composition named MVP9 presents the best chemical durability and cellular viability. The glass composition named MVP9b was considered the most promising material to produce microspheres because it has the best chemical durability and resistance to crystallization.

The loss of phosphorus during the glass processing does not prevent the final application of this material because the remaining amount is enough to achieve the required activity for radiotherapy applications.

## Acknowledgements

The authors acknowledge CNPq for granting a pos-doc scholarship and for the financial support (Project # 471712/2004-3), and Fapesp (Project # 05/53241-9). The authors are indebted to Dr. Sizue Rogero for the cytotoxicity tests, Mr Reinaldo Aparecido da Costa (IPEN-CCN) for the DTA analyses, and Ms Sandra M. Cunha (CCTM-IPEN) for the FTIR analyses.

## References

[1] G.J. Ehrhardt, D.E. Day, Nucl. Med. Bio. 14 (1987) 233.
[2] K.V. Stribley et al., J. Surg. Res. 34 (1983) 25.
[3] N. Araki, Y. Nagata, K. Fujiwara, T. Aoki, M. Mitsumori, H. Kimura, S. Itasaka, H. Saitou, M. Hiraoka, M. Kawashita, T. Kokubo Nucl, Int. J. Radiat. Oncol. Biol. Phys. 14 (2001) 459.
[4] M.J. Hyatt, D.E. Day, J .Am. Ceram. Soc. 70 (1987) 283.
[5] E.M. Erbe, D.E. Day, J. Biomed. Mater. Res. 27 (1993) 1301.
[6] R.C. Weast, D.R. Lide, M.J. Astle, W.H. Beyer, CRC Handbook of Chemistry and Physics, vol. B-28, CRC, Boca Raton FL, 1989. p. 231.
[7] R.V.P. Mantravadi, D.G. Spignos, W.S. Tan, E.L. Felix, Radiology 142 (1982) 783.
[8] M.J. Herba, F.F. Illescas, M.P. Thirlwell, L. Rosenthall, P. Smith, Radiology 169 (1988) 311.
[9] M.J. Herba, F.F. Illescas, M.P. Smith, Cancer 61 (1983) 1336.
[10] S. Houle, T.K. Yip, F.A. Shepherd, L.E. Rotstein, K.W. Sniderman, E. Theis, R.H. Cawthorn, K. Richmond-Cox, Radiology 172 (1989) 857.
[11] J.H. Anderson, J.A. Goldberg, R.G. Bessent, D.J. Kerr, J .H. Mckllop, I. Stewart, T.G. Cooks, C.S. Meardle, Radiotherapy Oncol 25 (1992) 137.
[12] M.A. Burton, B.N. Gray, C. Jones, A. Coletti, Nucl. Med. Biol. 16 (1992) 495.
[13] F.A. Shepherd, L.E. Lotstein, S. Houle, T.K. Yip, K. Paul, K.W. Sniderman, Cancer 70 (1992) 2250.
[14] D.E. Day, T.E. Day, An Introduction to Bioceramics, in: L.L. Hench, J. Wilson (Eds.), World Sconce, Singapore, 1993. p. 305.
[15] J.C. Andrews, S.C. Walker, R.J. Ackermann, L.A. Cotton, W.D. Newsmonger, B. Shapiro, J. Nucl. Med. 35 (1994) 1637.
[16] M. Kawashita, F. Miyaji, T. Kokubo, G. Takaoka, I. Yamada, Y. Suzuki, M. Ionue, J. Non-Cryst. Solids 255 (1999) 140.
[17] W. Huang et al., J. Shanghai Inst. Bldg. Mat. 4 (1992) 347.
[18] ISO document 10993-5. Biological evaluation of medical devices, Part 5, Tests for cytotoxicity: in vitro methods, 1992.
[19] S.O. Rogero, S.M. Malmonge, A.B. Lugão, T.I. Ikeda, L.L. Miyamaru, A.S. Cruz, Biocompatibility study of polymeric biomaterials, in: Proceedings do II COLAB – Congresso Latino-Americano de Órgãos Artificiais e Biomateriais, Belo Horizonte, Dezembro 200.
[20] S.T. Reis, M. Karabulut, D.E. Day, J. Non-Cryst. Solids 292 (2001) 150.
[21] X. Fang, C.S. Ray, G.K. Marasinghe, D.E. Day, J. Non-Cryst. Solids 263&264 (2000) 293.
[22] M. Karabulut, G.K. Marasinghe, P.G. Allen, C.H. Booth, M. Grimsditch, J. Mater. Res. 15 (2000) 1972.
[23] A.M. Efimov, J. Non-Cryst. Solids 209 (1997) 209.
[24] A. Hruby, Czech. J. Phys. B-22 (1972) 1187.
[25] Y. Abe, D.E. Clerk, J. Mater. Sci. Lett. 9 (1990) 244.
[26] W.M.Pontuschka, M. Sen, C.G. Rouse, Técnicas de preparação de vidros especiais, Apostila do curso de pós-graduação, IFUSP, 1992.